

RESEARCH

Open Access



Can quercetin reduce arsenic induced toxicity in mouse BALB/c 3T3 fibroblast cells? A study involving in vitro, molecular docking, and ADME predictions

Velid Unsal^{1*} , Cumali Keskin² and Erkan Oner³

Abstract

This study aimed to investigate the protective effect of quercetin against arsenic-induced oxidative damage, inflammation, and apoptosis in mouse BALB/c 3T3 fibroblast cells (NIH-3T3). Arsenic at different concentrations of 0.05 μM (low), 0.5 μM (medium), 10 μM (high) doses were used to induce toxicity, while 120 μM quercetin was used for treatment. MTT and LDH analyses were performed to determine the effect of arsenic and quercetin on cell viability, while oxidative stress markers and antioxidant enzyme activities were measured by spectrophotometric method. TNF- α and IL-1 β levels were measured by the ELISA method, Autodock programs were used for molecular docking studies. In addition, computer-based analyses of quercetin and succimer molecules were performed using SwissADME web tools. TNF- α (PDB ID: 2AZ5), IL-1 β (PDB ID: 1ITB), Caspase3 (PDB ID: 2XYG), Bax (PDB ID: 4S0O), SOD (PDB ID: 1CBJ), GSH-Px (PDB ID: 1GP1) and Bcl-2 (PDB ID: 1G5M) crystal structures were obtained from the Protein Data Bank. Bax and Bcl-2 levels of apoptotic genes and mRNA expression levels of Caspase-3 activity were measured using the QRT-PCR technique. TUNEL staining was performed to determine DNA fragmentations, while DAPI staining was done to visualise nuclear modifications. Quercetin has been found to significantly reduce oxidative stress, inflammation, and apoptosis in cells and exert anti-apoptotic effects. Molecular docking studies revealed quercetin shows good binding affinity with molecules with SOD, GSH-Px, Bax, Bcl-2, Caspase-3, TNF- α and IL-1 β structures, and has been observed to bind with Bax and Bcl-2 with molecular docking scores of -7.5 and -7.7 kcal/mol, respectively. These findings are supported by results showing that quercetin is effective in anti-apoptotic and anti-inflammatory processes in arsenic-induced cells under in vitro conditions. In addition, when ADME values are examined, it can be considered that quercetin is a useful and effective candidate compound in reducing arsenic toxicity, considering its higher synthetic accessibility score, better pharmacokinetic properties, and good biological transition and interaction capacities compared to succimer.

Keywords Arsenic toxicity, Quercetin, Succimer, Molecular docking, ADME

*Correspondence:

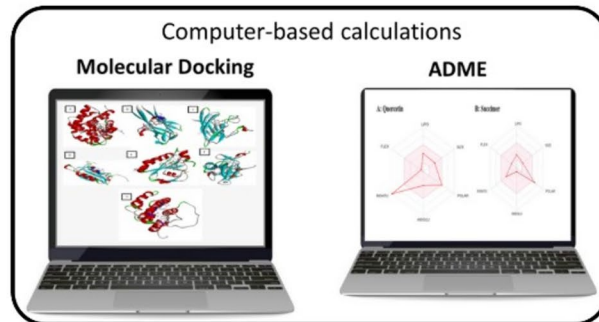
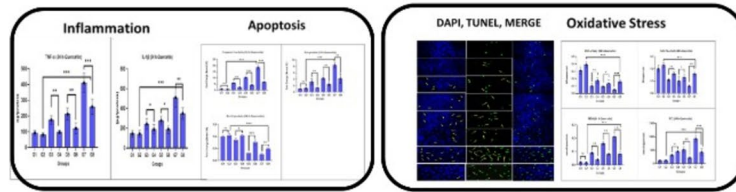
Velid Unsal
velidunsal@artuklu.edu.tr

Full list of author information is available at the end of the article



© The Author(s) 2025. **Open Access** This article is licensed under a Creative Commons Attribution-NonCommercial-NoDerivatives 4.0 International License, which permits any non-commercial use, sharing, distribution and reproduction in any medium or format, as long as you give appropriate credit to the original author(s) and the source, provide a link to the Creative Commons licence, and indicate if you modified the licensed material. You do not have permission under this licence to share adapted material derived from this article or parts of it. The images or other third party material in this article are included in the article's Creative Commons licence, unless indicated otherwise in a credit line to the material. If material is not included in the article's Creative Commons licence and your intended use is not permitted by statutory regulation or exceeds the permitted use, you will need to obtain permission directly from the copyright holder. To view a copy of this licence, visit <http://creativecommons.org/licenses/by-nc-nd/4.0/>.

Graphical Abstract



“
Quercetin is an important compound and ligand that has the potential to reduce toxicity by reducing ROS production in cells, increasing antioxidant capacity, and maintaining the balance of inflammation and apoptosis in cells.
 ”

- Arsenic**
 - Arsenic concentrations were decided. Arsenic concentrations of 0.05 μM (low), 0.5 μM (intermediate), 10 μM (high) doses were determined.
- Quercetin**
 - The optimal dose of quercetin was decided. It was decided that the optimal dose would be 120 μM quercetin.
- Oxidative Stress and Inflammation**
 - TNF-α and IL-1β were measured by ELISA method, while SOD, GSH-Px, MDA and PC parameters were studied by spectrophotometric method
- Apoptosis**
 - Expression measurement of genes (Bax, Bcl2, and Caspase 3) and Immunofluorescence images (DAPI, TUNEL)
- Computer-based calculations**
 - Molecular docking, ADME and Allergenicity

Introduction

NIH3T3 cells, or Mouse BALB/c 3T3 fibroblasts, are among the most popular cell lines in life science research and are used in many research laboratories around the world. One of the reasons why mouse BALB/c 3T3 fibroblasts are preferred in biological and toxicological studies is their susceptibility to oxidative stress, which is thought to play a role in cell death mechanisms, and in addition, mouse BALB/c 3T3 fibroblasts are more sensitive to toxic applications than human fibroblasts. Therefore, this cell line was preferred for the arsenic toxicity model [1–3]. The toxic heavy metal arsenic, is an element with the atomic number 33 belonging to the VA group in the periodic table. Arsenic is widely available and it is defined as a metalloid because it exhibits both metal and non-metal properties. Although arsenic pollution in drinking water is of natural origin, the use of herbicides, insecticides, rodenticides, preservatives, and by-products of fossil fuels, especially those containing arsenic, is also sufficient to challenge the aquatic environment and humanity. It originates from a wide range of industrial, chemical, residential, agricultural, and technological sources, leading to extensive contamination of aquatic, soil and air ecosystems, including flora, fauna, and humans. Arsenic is an important toxic substance in global and environmental problems, can affect the overall quality of life by causing various harmful effects on cells and organs. Exposure to arsenic changes, signal pathways and epigenetic modifications, induces the development of intracellular reactive oxygen species (ROS) leading to direct oxidative damage or oxidative stress in cells or molecules [4–12]. Arsenic induces the enhanced production of free radicals such as singlet oxygen (1O_2), superoxide radical anion ($O_2^{\cdot-}$), hydrogen peroxide (H_2O_2), hydroxyl radical ($\cdot OH$), and peroxy radical ($ROO\cdot$) [13]. Increased cellular ROS as a result of arsenic exposure leads to oxidative stress and therefore to DNA damage, cell death, and lipid peroxidation, as well as disrupting redox enzyme activities and antioxidant defence system [14–16]. In addition, exposure to arsenic can cause endothelial dysfunction and aggravation of cardiovascular pathology as it increases the expression of interleukin-1, tumor necrosis factor- α , vascular endothelial growth factor and vascular cell adhesion molecule [17]. Artificial intelligence and computational drug discovery have become an important approach that helps identify an efficient and effective drug molecule against various toxicities [18]. In recent years, large-scale data on hundreds of thousands of small molecules have been produced through biological screening, and many FDA-approved drugs have been developed because of these computational methods [19]. Since the environmental burden of heavy metals such as arsenic, is a growing concern, mitigating measures must be taken in this regard [20–21]. With the exception

of British anti-Lewisite (BAL), which contains two sulfhydryl and hydroxyl groups against arsenic nerve gas and is the first reported antidote, dimercaptopropanol-sulfonate (DMPS), meso-2,3-dimercaptosuccinic acid (DMSA), sodium 2,3, monoisoamyl DMSA (MiADMSA), monomethyl DMSA (MmDMSA), monocyclohexyl DMSA (MchDMSA), calcium disodium ethylenediamine tetraacetic acid ($CaNa_2EDTA$), calcium trisodium diethylenetriaminepentaacetate, D-penicillamine, tetraethylenetetraamine (TETA) or trientine, nitrilotriacetic acid (NTA), deferoxamine (DFO), deferiprone (L1) are the main chelate-forming agents reported to be effective against heavy metal toxicity [22–23]. DMSA or succimer, is an analogue of BAL and is an effective antidote. DMSA has several advantages over BAL, for example, it dissolves well in water, can be administered orally, and is less toxic [23–26]. Many researchers around the world have tested a large number of natural and synthetic chemicals/compounds for arsenic toxicity, both in vitro and in vivo. However, these natural and synthetic chemicals/compounds have failed to advance adequate evidence-based treatment regimens to improve the toxicity caused by arsenic [27–28]. Flavonoids are known worldwide for their antioxidant and radical scavenging activities due to their chelating activity that can be used in different conditions [29–31]. The primary flavonoid is quercetin, which is abundant in a wide variety of plants and is considered the leading molecule of the entire class of flavonoids [31]. Quercetin, which is found in almost all edible vegetables and fruits, is a natural polyphenolic flavonoid with (3,3',4',5,7 - pentahydroxyflavon) antioxidant and anti-inflammatory activities [32]. Gradually increasing evidence shows that due to its antioxidant effects, quercetin plays an important role in the prevention and treatment of cardiovascular and neurodegenerative diseases, osteoporosis, and certain cancer types. quercetin has various effects on various signal transmission pathways by activating, inhibiting, downregulating or upregulating many molecules in the body. quercetin balances oxidative stress by reducing or inhibiting oxidative stress arising from the imbalance between oxidants and antioxidants in the body [33–34]. Moreover, quercetin has antiallergic, antifungal, anti-inflammatory, antiseptic, antidiabetic, hepatoprotective, neuroprotective, and immunostimulant activities [35–37]. It is primarily necessary to understand the pathophysiological changes in BALB/c 3T3 fibroblast cells induced by arsenic and whether quercetin could correct these pathophysiological changes or not. Therefore, antioxidative agents such as quercetin may be a possible therapeutic approach to reduce/treat arsenic-exposed cell toxicity. Oxidative stress occupies a significant place in the arsenic toxicity mechanism. Therefore, this study aimed to understand the mechanism of arsenic-induced oxidative stress by using current antioxidant

treatments to identify suitable, safe, and specific treatments. The main purpose of the study was to gain insight into the toxicity of arsenic heavy metal in BALB/c 3T3 fibroblast cells, the effects of quercetin against arsenic toxicity, and the related molecular mechanism(s). In addition, the physicochemical properties, drug similarity, and ADME (absorption, distribution, metabolism, and excretion) parameters of succimer, which are routinely used in the investigation quercetin and arsenic toxicity, were also calculated. To the best of our knowledge, no such large-scale comparison has been made in the literature thus far, which indicates that the study is original.

Materials and methods

Chemicals

The standard arsenic solution (H_3AsO_4 , It is a compound in the form of As(V).) was purchased from Merck company (Germany), quercetin was purchased from Sigma-Aldrich Company (St. Louis, MO, USA), and other chemicals were procured from Acros Organics (Belgium) and Isolab (Germany). The chemicals were of analytical purity. In addition, all consumables were sterile.

Determination of the arsenic dose

Frozen BALB/c 3T3 fibroblast cells were thawed in culture medium, seeded in appropriate medium and grown. Cells were grown in 5% CO_2 at 37 °C, in standard DMEM culture medium and in medium containing 10% fetal bovine serum. Cells were routinely passaged with 0.25% trypsin-EDTA solution and cell density was monitored at each passage until 80–90% confluency was reached. Cells were plated at 10,000 cells per well. This application was determined to be a level at which cell density and cells could be observed more accurately. In our study, the H_3AsO_4 compound was preferred because it has the potential to convert As(V) to As(III) in the cell and provides a more stable and controlled environment under laboratory conditions. Then, different concentrations of arsenic (from 0.001 μM to 10 μM) were applied to the cells, and the MTT test (Biotium, MTT cell viability test kit, Catalog No: 30006) was used to measure cell viability. After 24 h, 10 μl of MTT solution was added to each well and kept at 37 °C for 4 h. Then, 200 μl of DMSO was added to each well to dissolve the formazan crystals in the cells and absorbance values were measured at a wavelength of 570 nm. By subtracting the absorbance values of the blind wells, the viability of the control group was accepted as 100% and the viability percentages of the arsenic-treated groups were calculated. As a result of the evaluations obtained from cell viability, the most appropriate arsenic concentrations were determined for three different doses. Based on cell viability percentage calculations, doses of 25% (0.05 μM , low), 50% (medium, 0.5 μM , medium) and 75% (high, 10 μM) were determined.

Optimal quercetin dose

In order to determine the optimum dose for quercetin, Biotium brand MTT Cell Viability Analysis Kit (Catalog No: 30006) was used. The cells were planted in 96-well plates as 1×10^4 cells/wells and expected to be attached to the vial surface. Then, predetermined quercetin concentrations (40 μM , 80 μM , 120 μM) were applied to the cells. At the specified time points (hours 6, 12, 24, 48, and 72), 10 μl of MTT solution was added to each well and incubated for 4 h at 37 °C. Upon completion of the incubation process, 200 μl of DMSO was added to each well to dissolve the formazan crystals and absorbance values were measured at a wavelength of 570 nm. Using the data obtained, a graph showing the relationship between cell viability rates and quercetin concentrations was created. The optimum quercetin dose was calculated separately for each time point (6, 12, 24, 48 and 72 h). As a result of the analysis, it was determined that the optimum quercetin concentration for the cells was 120 μM .

Determination of lactate dehydrogenase (LDH) activity

In order to evaluate the cytotoxic effect of arsenic in the presence of quercetin, the LDH Cytotoxicity Detection Kit (Catalog No: CTG-CT0001) of Celltechgen LLC was used. LDH enzyme activity was determined by absorbance measurements at 490–492 nm wavelengths with ELISA reader device. These measurements were made in accordance with the kitin protocol.

Determination of the apoptotic effect of arsenic in the presence of Quercetin

ABP Bioscience's TUNEL Andy Fluor™ 488 Apoptosis Detection Kit (Catalog No: A050) was used. After performing the TUNEL assay, apoptotic cells were detected by inverted fluorescence microscope (Euromex OX.2253-PLF). Apoptotic index (%) was calculated by multiplying the ratio of apoptotic cell number to total cell number by 100: Apoptotic index (%) = (Apoptotic Cell Number / Total Cell Number) \times 100.

Real-time quantitative polymerase chain reaction (RT-qPCR)

Total RNA was isolated from cells using a kit (GeneAll, Hybrid-R, Cat No: 305–101). Total RNA was reverse-transcribed into complementary DNA (cDNA) using the First Strand cDNA Synthesis Kit (Wizbio, WizScript™ cDNA Synthesis Kit (High Capacity) W2211). After obtaining the cDNA Real-Time qPCR reaction (Wizbio, WizPure™ qPCR Master (SYBR) Catalog No: W1711) was initiated. The reaction conditions for Real-Time qPCR were as described in the leaflet of the kit. The primary information used in the expression analysis is given (Table 1). Quantification of Bax, Bcl2 and Caspase 3, GAPDH mRNA expression levels, real-time qPCR was

Table 1 List of QRT-PCR primers

Primer	Nucleotide sequence (5'-3') forward	Nucleotide sequence (5'-3')-reverse	Synthesizing firm
Bax	TGAAGACAGGGCCCTTTTG	AATTCGCCGGAGACTCTCG	Oligomer
Bcl-2	ATGCCTTTGTGGAACATATGGC	GGTATGCACCCAGAGTGATGC	Oligomer
Caspase-3	ATGGAGAACAACAAAACCTCAGT	TTGCTCCCATGTATGGTCTTTAC	Oligomer
GAPDH	TGACCTCAACTACATGGTCTACA	CTCCCATCTCTCGGCCTTG	Oligomer

performed using an Applied Biosystems™ 7500 Fast Real-Time PCR device. The quantitation of RNA expressions was normalised to the control group using the GAPDH transcript as a reference. The “ $\Delta\Delta C_t$ Method” was used in the relative quantification calculation.

Biochemical measurements

The cells seeded in culture flasks at the end of the experimental applications (1×10^6 cells per well) were removed and suspended to Tris-HCl tampon (pH 7. 2). Then, cell membrane were defragmented by sonicating them with an ultrasonicator, and the cell suspension obtained was centrifuged at 14,000 g at a coolant centrifuge for 10 min and the supernatant was collected. From the supernatants, TNF- α (Cat.No E0764Ra) and IL-1 β (Cat.No E0119Ra) were measured by the ELISA method according to the kit instructions. From the supernatants, the antioxidant enzymes of superoxide dismutase (SOD), glutathione peroxidase (GSH-Px), lipid peroxidation (MDA), and protein carbonyl (PC) were studied. SOD activity was determined with the method of Sun et al. and GSH-Px activity was determined with the method of Paglia and Valentine [38–39]. While MDA was determined with a method based on the reaction with thiobarbituric acid (TBA) at 90–100 °C, The PC was determined spectrophotometrically to form 2,4-dinitrophenylhydrazone based on the reaction of the carbonyl group with 2,4-dinitrophenylhydrazine [40–41]. Protein measurements of the supernatants were performed using the Lowry method [42].

Molecular docking analysis

Ligand system

Quercetin was retrieved from PubChem using the sdf format (<https://pubchem.ncbi.nlm.nih.gov/>). Converted from Open Babel GUI program to pdb format.

Protein system

TNF-alpha (PDB ID: 2AZ5), IL-1 β (PDB ID: 1ITB), Caspase 3 (PDB ID: 2XYG), Bax (PDB ID: 4S0O), SOD (PDB ID:1CBI), GSHpx (PDB ID: 1GP1) and Bcl-2 (PDB ID: 1G5M) crystal structures were obtained from the Protein Data Bank (www.rcsb.org). Fibroblast cell were retrieved from the protein database (PDB ID: 6M6E).

Molecular docking

Autodock 4.2.6 is used. To improve the more precise estimation of the ligand pose in the pockets of the targets as well as the determination of binding energies present in the generated DLG files, all resulting complexes were docked in duplicate using Autodock 4.2 [43]. Not only does Autodock 4.2 have the scoring function that uses the AMBER force field to estimate the binding energy of the ligand receptor, but AutoDock 4.2 also uses the Lamarckian Genetic Algorithm (LGA) [44]. Active sites were entered and a grid parameter file was created for each protein by fixing the number of grid points in the x, y, and z axes to $80 \times 80 \times 80$ with a grid spacing of 0.375 Å. Deployment parameters: number of energy evaluations set to 250,000 and number of generations set to 50. Another important point to remember was that other docking parameters were set to the software's default values [45]. AutoGrid 4.2 and AutoDock 4.2 programs were used to prepare grid maps, create digital line graph (DLG) files and obtain molecular placement results. During the gross insertion procedures, conformers with the lowest root mean square deviation (RMSD) values and high negative binding energies for quercetin and metal (Arsenic) interactions were selected from among 50 different conformers produced as a result of genetic algorithm-based studies. The Discovery Studio 2019 program was used for the visualization and analysis of the obtained interlocked conformations at the molecular level [46]. A docking model with metal (Arsenic) was created only for PDB ID: 6M6E. In addition to the above method, the parameters required for Arsenic were added to the parameter_file AD4_parameters.dat file.

ADME and allergenicity

The SwissADME web server was used, which assists medical pharmacologists and chemists in predicting the pharmacokinetic and drug similarity properties of various substances, leading to the discovery, development and optimization of new drugs. (<http://www.swissadme.ch/>, access date January 13, 2024) [30, 47]. The canonical SMILES (Simplified Molecular Line Entry System) of both compounds were provided to the presenters to calculate the relevant properties. The allergenicity of selected quercetin and succimer was predicted using the CHAIred server (<https://webs.iitd.edu.in/raghava/chalpred/>, access date January 15, 2024). Small inhibitors can

Table 2 Cell viability at different arsenic concentrations

Arsenic (24 h) (μM)	Mean	SD
0	100.000	4.814
0.001	99.712	3.024
0.01	89.817	8.321
0.02	83.477	4.961
0.05	76.721	4.551
0.1	66.218	6.171
0.2	62.120	7.701
0.5	54.243	7.978
1	46.910	4.994
2	41.467	3.053
5	32.053	7.722
10	27.185	3.329

elicit immune responses after binding to specific protein [48, 49].

Statistical analysis

Statistical analyses were performed using GraphPad Prism 9.2 (GraphPad Software, Inc., San Diego, CA) and SPSS (IBM SPSS Statistics 22, SPSS Inc.) package program. Descriptive statistics were used to provide information about the general characteristics of the groups. The results are expressed as mean \pm standard deviation (SD). The normality distribution was evaluated using the Shapiro-Wilk test, while the homogeneity of the variances was tested by the Levene test. ANOVA was used for normally distributed data, and Kruskal-Wallis test was used for non-normally distributed data for continuous variable comparisons of more than two independent groups. Post-hoc Tukey-Kramer test were used for further comparisons. $p < 0.05$, ** $p < 0.01$, and $p^{***} < 0.001$ were considered statistically significant.

Results

Cell viability at different arsenic concentrations

In the evaluations, the closest or appropriate values for cell viability were determined as 25% (0.05 μM , lowest), 50% (0.5 μM , medium), and 75% (10 μM , highest) doses (Table 2). When we examined the effect of different doses of quercetin at different times on cell viability, we determined increased cell viability at different times compared with the control group. The highest effect was observed at a dose of 120 μM at 24 h. Thus, the most suitable dose was 120 μM (Fig. 1). In the study, three different doses of (low, medium, high) (0.05 μM , 0.5 μM , and 10 μM) arsenic concentrations were used for cell viability. LDH activities of the groups (G3, G5, G7) that were administered only arsenic (low, medium an, high) significantly increased ($p < 0.05$). The highest LDH activity among these three groups was observed in group G7 ($p < 0.001$). As a result of the treatment of the groups that were administered three different doses of arsenic (G4, G6, G8) with quercetin (120 μM), the LDH activities of these three groups significantly decreased (Fig. 2).

Arsenic increases ROS oxidative stress factors, whereas quercetin decreases arsenic-induced oxidative stress

SOD and GSH-Px activities of low (G3), medium (G5) and high dose (G7) arsenic-treated groups decreased significantly. The lowest SOD and GSH-Px activities were observed in G7 group among these three groups ($p < 0.001$). However, with quercetin treatment, it was observed that the activities of SOD and GSH-Px enzymes of groups (G4, G6, and G8) increased significantly (Fig. 3A and B). MDA and PC levels increased significantly only in arsenic-treated groups (G4 low, G6 medium and G8 high dose) ($p < 0.05$) and the highest MDA and PC levels were in G8 group among these three groups ($p < 0.001$). However, MDA and PC levels decreased with quercetin treatment. It showed a significant positive change (Fig. 3C and D).

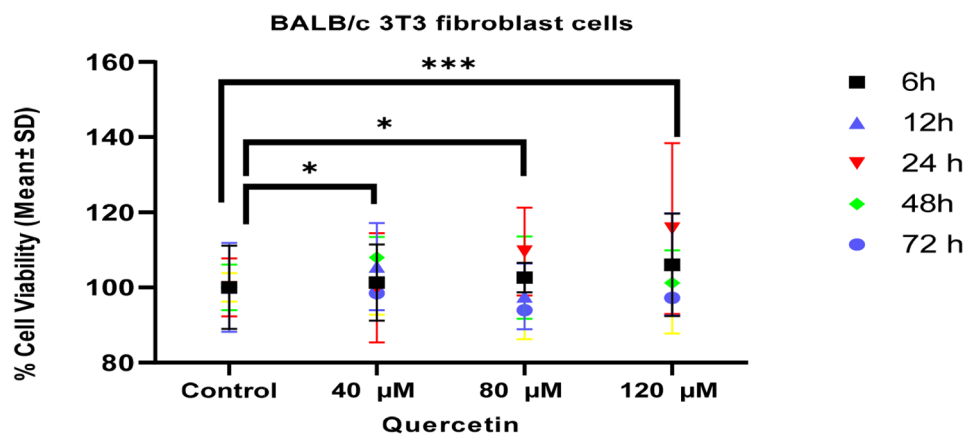


Fig. 1 The effect of different doses of quercetin at different times on cell viability

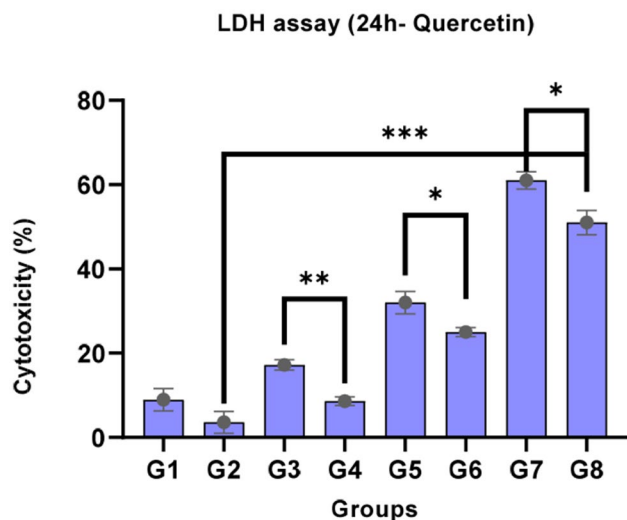


Fig. 2 LDH activity of the groups. Data represents mean * $p < 0.05$, ** $p < 0.01$, *** $p < 0.001$. G1: Control, G2: Quercetin 120 μ M, G3: 0.05 μ M Arsenic G4: 0.05 μ M Arsenic + Quercetin 120 μ M G5: Arsenic 0.5 μ M G6: Arsenic 0.5 μ M + Quercetin 120 μ M, G7: 10 μ M Arsenic G8: 10 μ M Arsenic + Quercetin 120 μ M

Quercetin reduces arsenic-induced inflammation

Only arsenic-administered groups (low (G3), medium (G5), and high dose (G7), respectively) had significantly increased TNF- α and IL-1 β levels. Among these three groups, the highest TNF- α and IL-1 β levels were observed in group G7 ($p < 0.001$, $p < 0.01$, respectively). TNF- α and IL-1 β levels in groups (G4, G6, G8) administered quercetin for treatment purposes decreased significantly (Fig. 4A and B).

Quercetin reduces arsenic-induced apoptosis

Caspase-3 mRNA expression and Bax protein mRNA expression levels were significantly increased in only arsenic-treated groups (G3, G5, G7) ($p < 0.05$). Among these three groups, the highest caspase-3 mRNA expression and Bax protein mRNA expression levels were observed in the G7 group ($p < 0.001$ and $p < 0.01$, respectively). As a result of treatment with quercetin (120 μ M) in three different doses of arsenic-treated groups (G4, G6, G8), caspase-3 mRNA expression and Bax protein mRNA expression levels of these three groups increased ($p < 0.05$). (Fig. 5A and B) Bcl-2 mRNA levels (low, medium and high doses) in only arsenic-treated

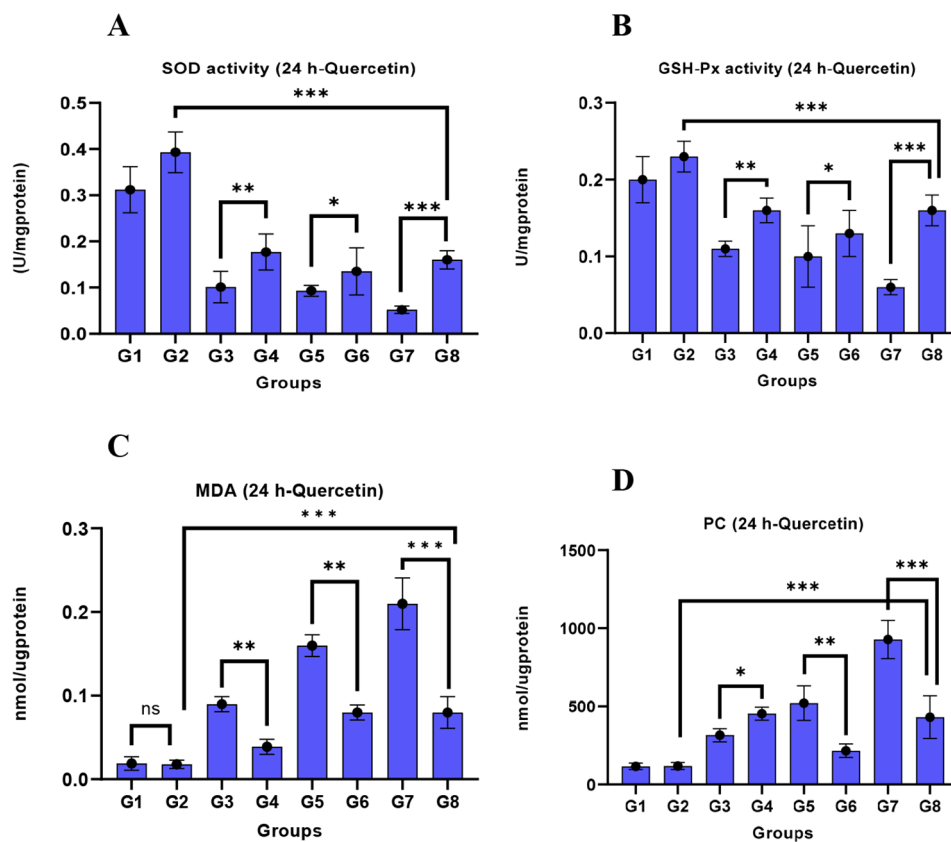


Fig. 3 SOD activity of groups (A), GSH-px activity of the groups (B), MDA level of groups. (C), PC level of groups (D) Note Data represents mean * $p < 0.05$, ** $p < 0.01$, *** $p < 0.001$. G1: Control, G2: Quercetin 120 μ M, G3: 0.05 μ M Arsenic G4: 0.05 μ M Arsenic + Quercetin 120 μ M G5: Arsenic 0.5 μ M G6: Arsenic 0.5 μ M + Quercetin 120 μ M, G7: 10 μ M Arsenic G8: 10 μ M Arsenic + Quercetin 120 μ M

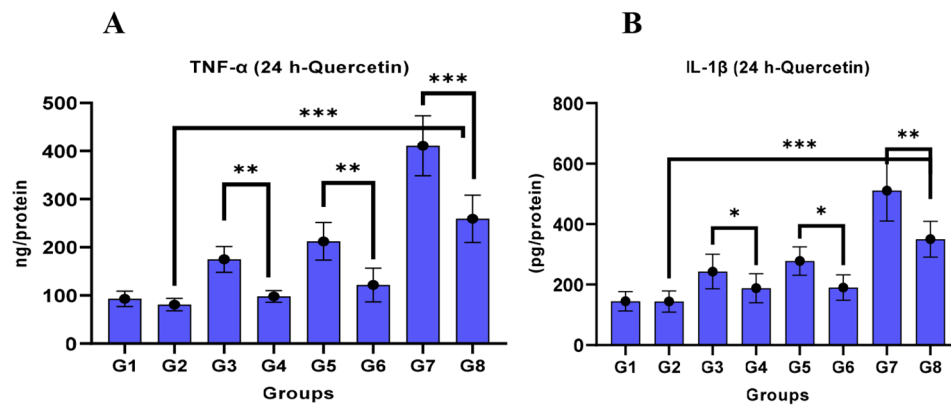


Fig. 4 TNF- α levels of the groups (A) IL-1 β levels of the groups (B) Note Data represents mean * $p < 0.05$, ** $p < 0.01$, *** $p < 0.001$. G1: Control, G2: Quercetin 120 μ M, G3: 0.05 μ M Arsenic G4: 0.05 μ M Arsenic + Quercetin 120 μ M G5: Arsenic 0.5 μ M G6: Arsenic 0.5 μ M + Quercetin 120 μ M, G7: 10 μ M Arsenic G8: 10 μ M Arsenic+ Quercetin 120 μ M

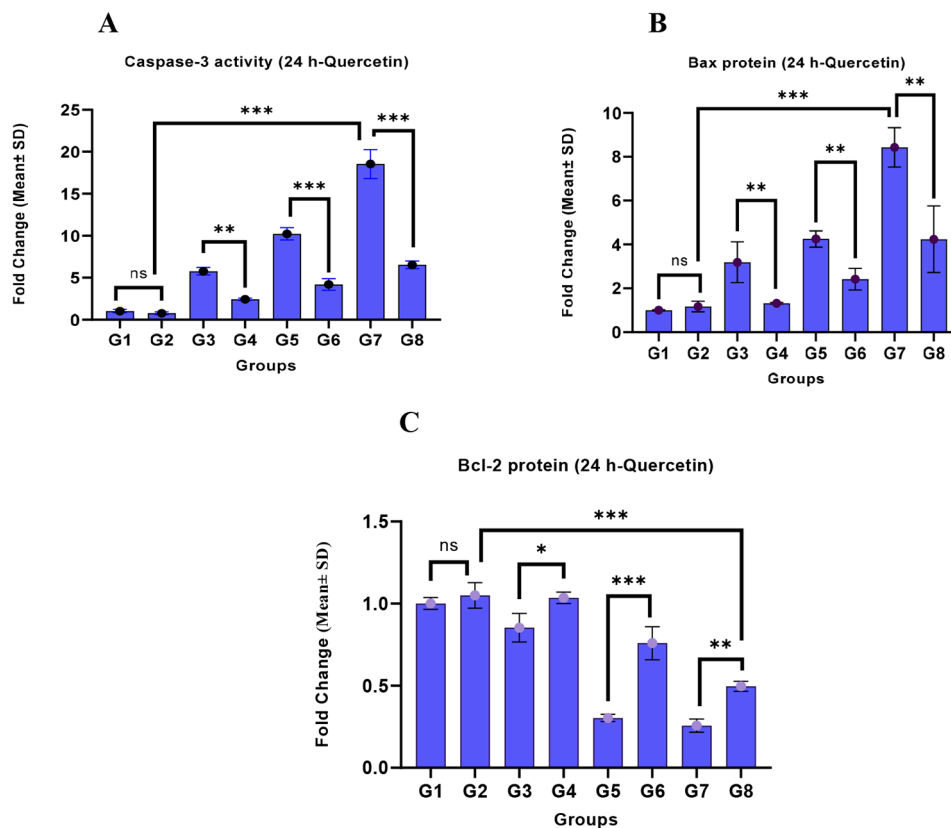


Fig. 5 Quantitative RT-PCR analysis of change in different doses of arsenic and quercetin. Expression of mRNA of caspase-3 activity of the groups. (A) Bax mRNA expression levels of the groups (B) Bcl-2 mRNA expression levels of the groups (C) Data represents mean * $p < 0.05$, ** $p < 0.01$, *** $p < 0.001$. G1: Control, G2: Quercetin 120 μ M, G3: 0.05 μ M Arsenic G4: 0.05 μ M Arsenic + Quercetin 120 μ M G5: Arsenic 0.5 μ M G6: Arsenic 0.5 μ M + Quercetin 120 μ M, G7: 10 μ M Arsenic G8: 10 μ M Arsenic+ Quercetin 120 μ M

groups (G3, G5, G7) decreased significantly. Among these three groups, the lowest Bcl-2 mRNA expression level was observed in the G7 group. As a result of treatment with quercetin (G4, G6, G8) in the groups that were administered three different doses of arsenic, the Bcl-2 mRNA expression levels of these three groups increased (Fig. 5C).

To better understand cell death, DAPI was used to understand the general morphology of cell nuclei and TUNEL was used to detect DNA fragmentation in apoptotic cells. MERGE was performed to see both nuclei and DNA fragmentation of apoptotic cells at the same time. The number of apoptotic cells was the lowest in G1 and G2 groups. TUNEL positive cells were almost absent. In

G3, G5 and G7 groups, the number of TUNEL positive cells increased significantly and gradually as the arsenic concentration increased. Nuclear shrinkages specific to apoptosis occurred in the cells. These shrinkages were observed in G5 and G7 groups. More limited effectiveness was observed in reducing the number of apoptotic cells even at different arsenic concentrations with quercetin treatment. This limitation was observed more in G8 group (Fig. 6A). When the apoptotic index of the groups was evaluated, the apoptotic index increased as the arsenic concentration increased. The group with the highest apoptotic index was G7 group. It was not significant for

G1 and G2. The apoptotic index decreased significantly in groups G4, G6 and G8 with quercetin treatment (Fig. 6B).

Molecular docking results

The fibroblast cell protein structure PDB ID: 6M6E and molecular docking results between quercetin and arsenic are given (Fig. 7; Table 3).

Our molecular docking results; A: Binding model of the quercetin compound in the Bax protein structure, B: Binding model of the quercetin compound in the TNF-alpha protein structure, C: Binding model of the quercetin compound in the SOD protein structure, D: Binding model of the quercetin compound in the

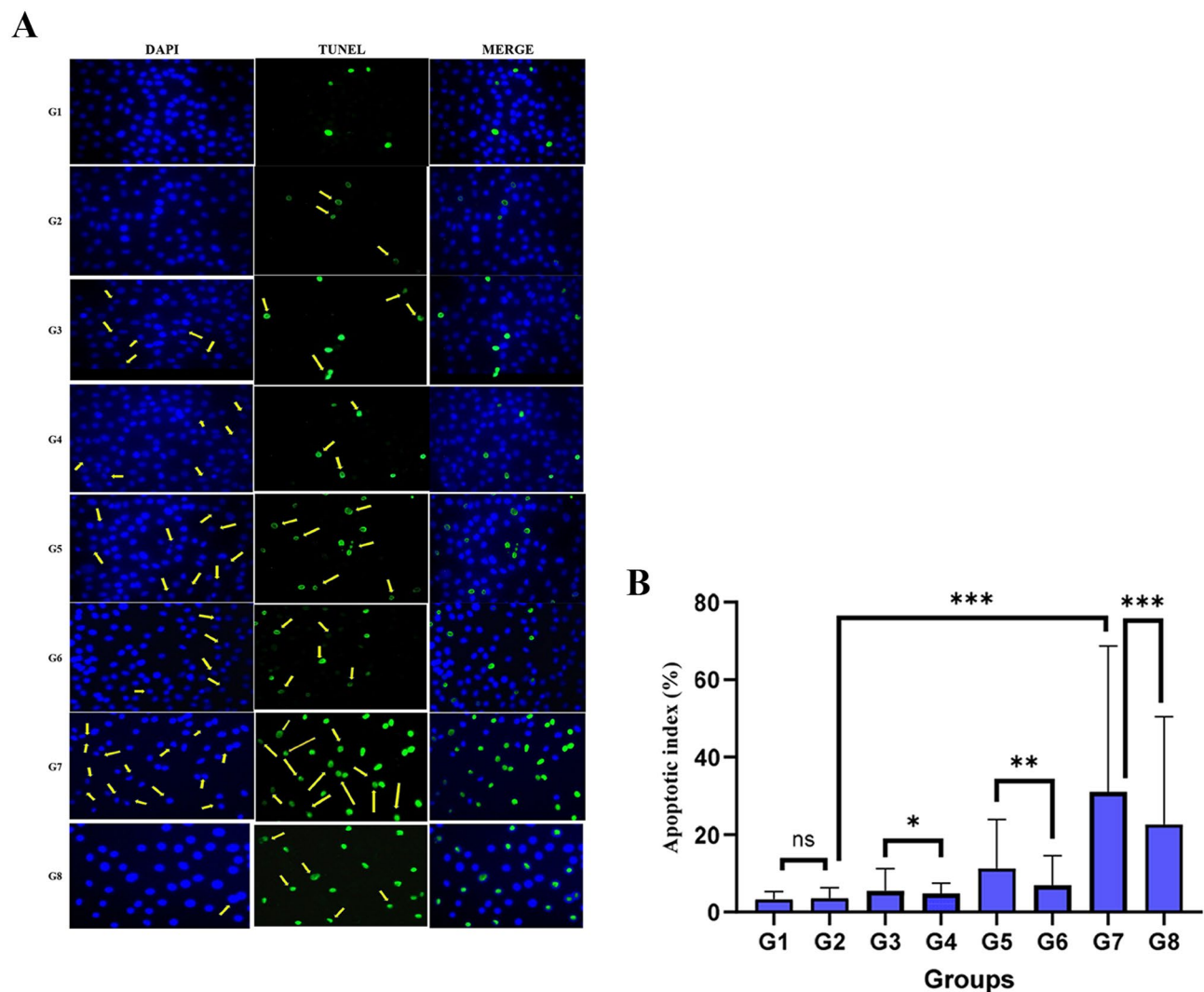


Fig. 6 Effects of arsenic exposure on post-treatment apoptosis with quercetin. DAPI (blue): nuclei; TUNEL (Green): DNA fragments after apoptosis; combining: overlapping cells. Magnification, $\times 400$. **TUNEL Top:** Evaluation of apoptosis in fibroblast cells was examined by DAPI staining (magnification, $200\times$) **Middle:** DNA fragmentation was detected by TUNEL assay (magnification, $400\times$). TUNEL-positive nuclei due to DNA fragmentation appear green in color. **Bottom:** Merged images of DAPI staining and TUNEL for the same area **G1:** Control, **G2:** Quercetin 120 μM , **G3:** 0.05 μM Arsenic **G4:** 0.05 μM Arsenic + Quercetin 120 μM **G5:** Arsenic 0.5 μM **G6:** Arsenic 0.5 μM + Quercetin 120 μM , **G7:** 10 μM Arsenic **G8:** 10 μM Arsenic+ Quercetin 120 μM . **B** Apoptotic index in different groups. Note: * $p < 0.05$, ** $p \leq 0.01$, *** $p \leq 0.001$ (mean \pm SD, $n = 3$), **G1:** Control, **G2:** Quercetin 120 μM , **G3:** 0.05 μM Arsenic **G4:** 0.05 μM Arsenic + Quercetin 120 μM **G5:** Arsenic 0.5 μM **G6:** Arsenic 0.5 μM + Quercetin 120 μM , **G7:** 10 μM Arsenic **G8:** 10 μM Arsenic+ Quercetin 120 μM

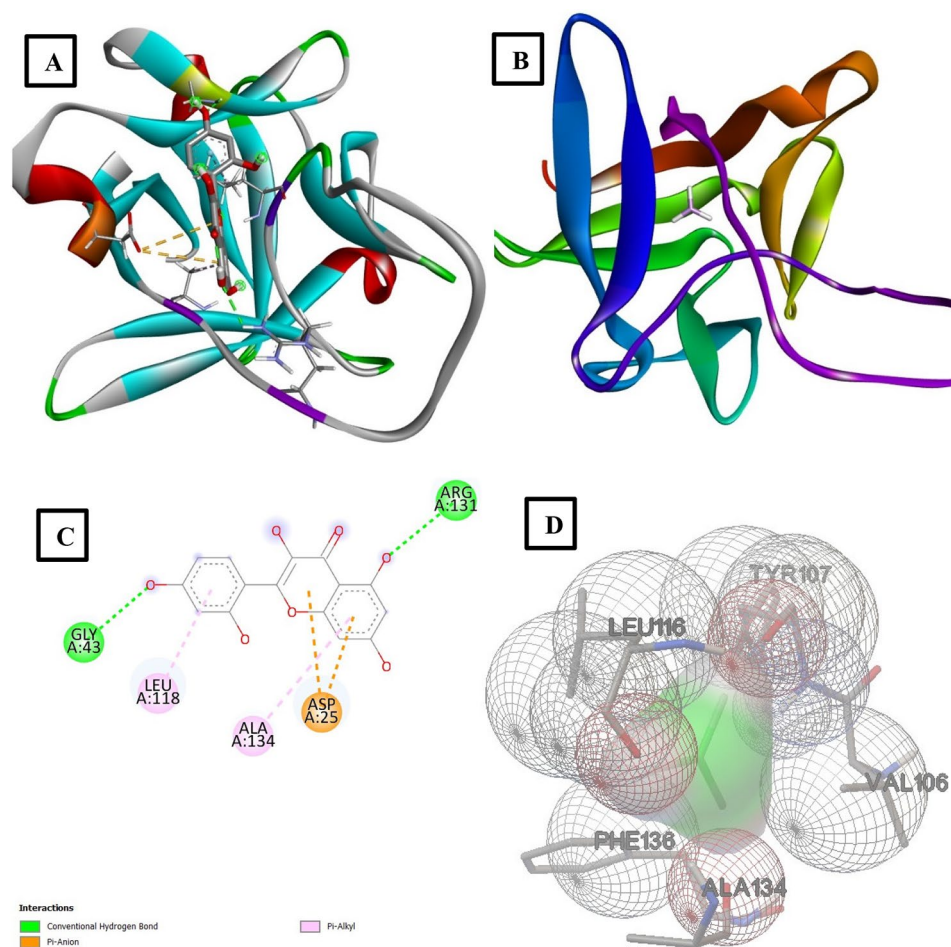


Fig. 7 Molecular docking results between quercetin and arsenic with fibroblast cells **A:** Molecular docking between quercetin and fibroblast cells, **B:** Molecular docking between arsenic and fibroblast cells, **C:** Amino acid bonding structures between fibroblast cell and quercetin **D:** Amino acid bond structures between fibroblast cell and arsenic.

Table 3 Amino acid bonding structures and docking scores between fibroblast cell and arsenic and Quercetin

Protein ID	Ligand	Docking score(kcal/mol)	Amino acid residue
6M6E	Quercetin	-6.6	ASP25, GLY43, LEU118, ARG131, ALA134
6M6E	Arsenic	-2.4	VAL106, TYR107, LEU116, ALA134, PHE136

Caspase-3 protein structure, **E:** Glutathione Peroxidase model of the quercetin compound. Binding model in the protein structure, **F:** The binding model of the quercetin compound in the IL- β protein structure, **G:** The binding model of the quercetin compound in Bcl-2 protein structure is presented (Fig. 8). Chemical bond interactions of quercetin with protein target structures have been demonstrated (Fig. 9). Molecular insertion scores and amino acid residues are shown in the protein target structures of quercetin (Table 4).

ADME and allergenicity

Quercetin passed Lipinski's rule of 5 completely, Ghose, Veber and Egan rules whereas succimer failed to pass Ghose (atom < 20), Veber (TPSA > 140) and Egan rules (TPSA > 131.6). The synthetic accessibility value of succimer was found to be 2.66 while that of quercetin was found to be 3.23. This value is interpreted that the closer to 1, the easier it is to synthesize a substance and the closer to 10, the more difficult it is to synthesize. The Log Po/w values of quercetin and succimer were below 5. This indicates that both the compounds have good permeability and absorption through the cell membrane (Fig. 10; Table 6). In addition, the solubility of a molecule is a critical factor that significantly affects the absorption of the compound during the formulation process. The Num. The value of H-bond donors was 5, while the value of succimer was 2. The value of H-bond acceptors was 7, while the value of succimer was 4. The expected MW value of quercetin between 80 and 480 was 302.24, while the MW value of succimer was 182.22. When the

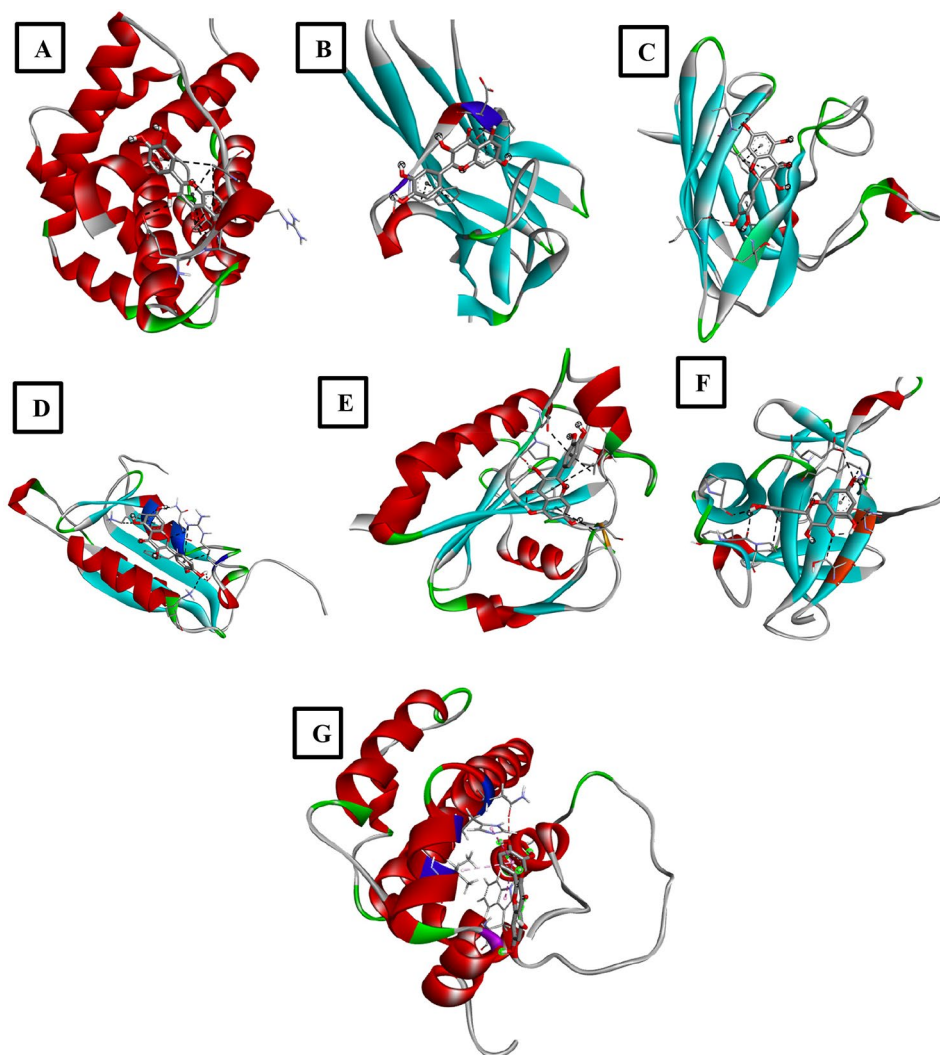


Fig. 8 Molecular docking results; **A:** Binding model of the quercetin compound in the Bax protein structure, **B:** Binding model of the quercetin compound in the TNF- α protein structure, **C:** Binding model of the quercetin compound in the SOD protein structure, **D:** Binding model of the quercetin compound in the Caspase-3 protein structure, **E:** Binding model of the GSH-Px model of the quercetin compound protein structure, **F:** Binding model of the quercetin compound in the IL-1 β protein structure, **G:** Binding model of the quercetin compound in the Bcl-2 protein structure

desired TPSA values between 20 and 130 Å² were examined, the TPSA value of quercetin was 131.36 Å², while the TPSA value of succimer was 152.20 Å (Table 6) [47]. When the allergenicity scores were examined, quercetin was 0.21 and succimer was 0.3. quercetin and succimer were found to be non-allergenic [49]. (Table 7).

Discussion

This study aimed to investigate the therapeutic effects of quercetin against arsenic-induced oxidative damage, inflammation and apoptosis in BALB/c 3T3 embryonic fibroblast cells. On the other hand, it was the first to elucidate how existing arsenic toxicity affects inflammatory processes and apoptotic mechanisms in BALB/c 3T3 embryonic fibroblasts and the effects of quercetin used for therapeutic purposes on these mechanisms. First,

arsenic, a source of toxicity or ROS, was administered, followed by quercetin. Our findings will provide a basic understanding for future research in environmental and medical fields due to the positive role of quercetin on oxidative damage, inflammation and apoptosis. In our molecular docking study, the main objectives of arsenic and quercetin in fibroblast cell targets were to understand and predict molecular recognition both structurally (finding possible binding modes) and energetically (estimating binding affinity). That is, the binding modes and affinity of arsenic and quercetin to fibroblast cell protein structure were estimated. SOD and GSH-Px levels of groups were examined to determine the protective role and antioxidant power of quercetin, and MDA and PC levels of groups were measured to determine arsenic-induced oxidative stress. mRNA expression levels of

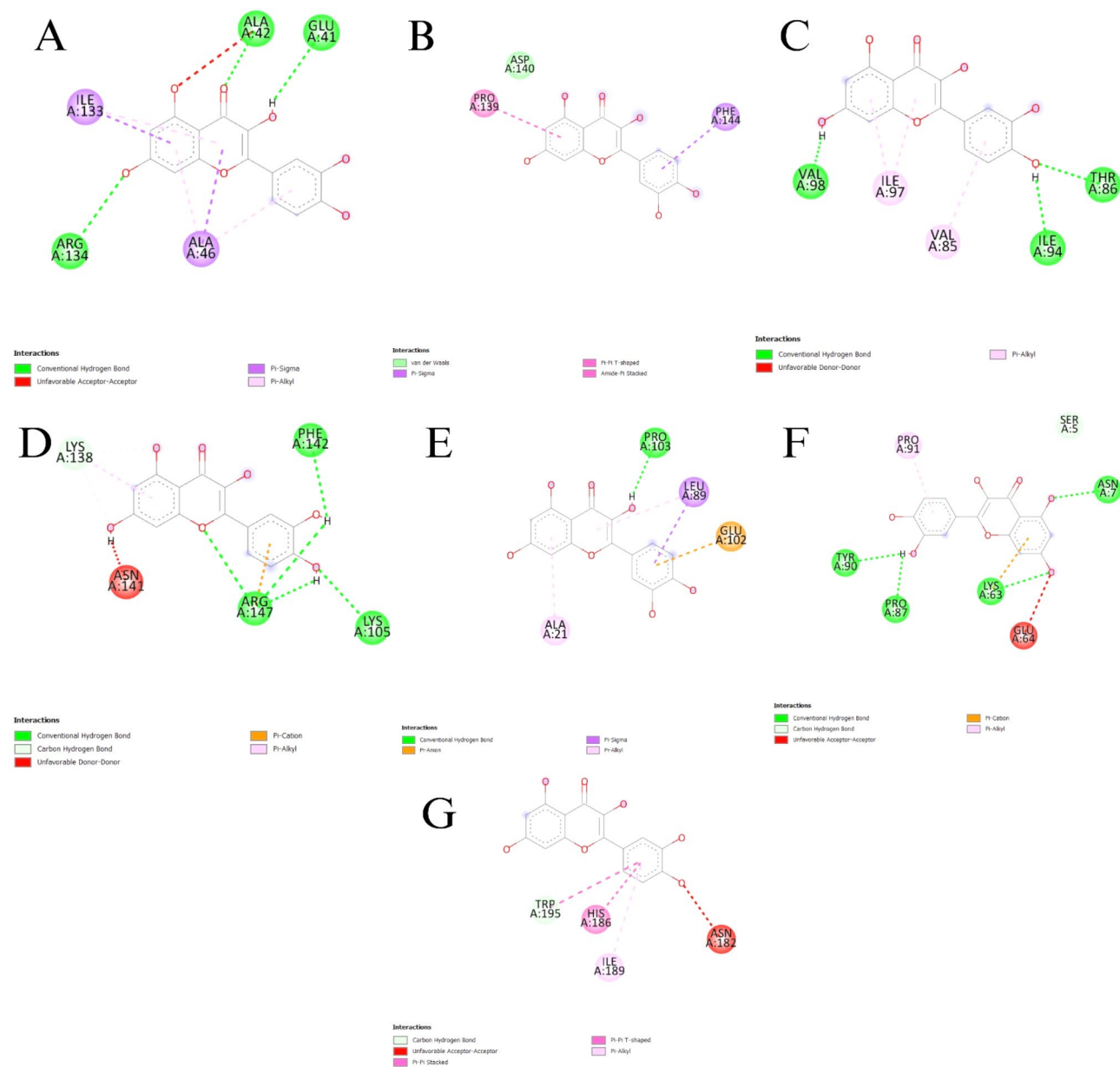


Fig. 9 Chemical bond interactions of quercetin with protein target structures; **A:** Binding model of the quercetin compound in the Bax protein structure, **B:** Binding model of the quercetin compound in the TNF- α protein structure, **C:** Binding model of the quercetin compound in the SOD protein structure, **D:** Binding model of the quercetin compound in the Caspase-3 protein structure, **E:** Binding model of the GSH-px model of the quercetin compound protein structure, **F:** Binding model of the quercetin compound in the IL- β protein structure, **G:** Binding model of the quercetin compound in the Bcl-2 protein structure)

Table 4 Molecular docking scores and amino acid residues of Quercetin's protein target structures were shown

Protein ID	Ligand	Docking Score(kcal/mol)	Amino Acid Residue
4S00-Bax	Quercetin	-7.5	ALA41, ALA42, ALA46, ILE133, ARG134
2AZ5-TNF- α	Quercetin	-6.6	PRO139, ASP140, PHE144
1CBJ-SOD	Quercetin	-6.6	VAL85, THR86, ILE94, ILE97, VAL98
2XYG-Caspase-3	Quercetin	-6.2	LYS105, LYS138, ASN141, PHE142, ARG147
1GP1- Glutathione Peroxidase	Quercetin	-6.8	ALA21, LEU89, GLU102, PRO103
1ITB-IL- β	Quercetin	-6.2	SER5, ASN7, LYS63, GLU64, PRO87, TYR90, PRO91
1G5M-Bcl-2	Quercetin	-7.7	ASN182, HIS186, ILE189, TRP195

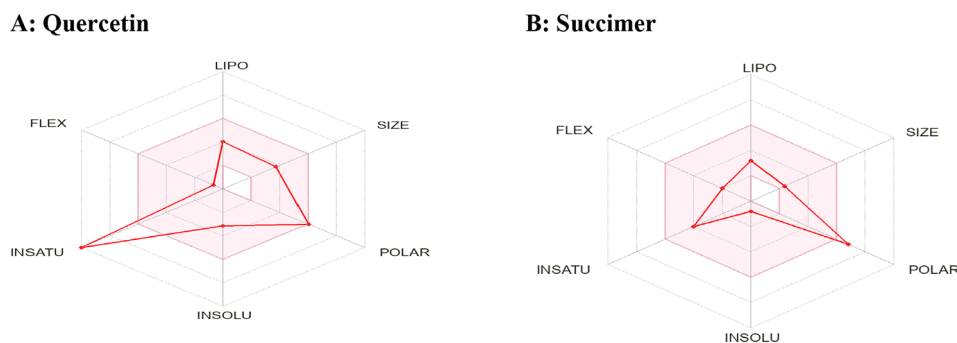


Fig. 10 Radar map of the quercetin and succimer molecule taken from the Swissadme database

Bax and Bcl-2 and mRNA expression levels of Caspase-3 activity of groups were measured to evaluate the effect of arsenic on apoptosis and the anti-apoptotic effect of quercetin. TNF- α and IL-1 β levels were measured to evaluate the effect of arsenic and quercetin on the inflammatory process. In addition, computer-based analyses of quercetin used for treatment and succimer molecules routinely used in heavy metal poisoning were performed and compared. As a result of the study, it was found that quercetin was protective against arsenic-induced toxicity in fibroblast cells and quercetin had some important advantages over succimer. Millions of individuals are affected exposure to arsenic [50]. It has been claimed in studies conducted that arsenic-induced free radicals and oxidative stress play a role in many diseases (various cancer types, cardiovascular diseases, neurological disorders, diabetes, etc.). Therefore, it is believed that antioxidant applications that eliminate free radicals and decrease oxidative stress can be effective against arsenic-induced toxicity [6, 50–52]. LDH, a stable cytoplasmic enzyme, is secreted by damaged cells and is considered an indicator of apoptosis, necrosis, and other cellular damage [53]. In this study, we determined that different concentrations of arsenic decreased cell viability in the BALB/c 3T3 fibroblast cell line, whereas quercetin (120 μ M) increased cell viability. In addition, arsenic increased LDH activity, whereas quercetin decreased LDH activity (Fig. 2). There are several studies on the effects of arsenic on cell viability in BALB/c 3T3 cells and different cell lines. Our findings are consistent with other *in vitro* studies that demonstrated that exposure to arsenic significantly decreased cell viability and increased LDH activity in embryonic fibroblasts and different cell lines [54–57]. In one study, the protective effect of quercetin against H₂O₂-induced cytotoxicity in H₂O₂-induced PC-12 cells was investigated. It was reported as a result of the MTT test that quercetin pretreatment significantly increased cell viability compared to the cells treated with H₂O₂, while quercetin decreased LDH release [58]. SOD and GSH-Px are the major members of the enzymatic antioxidant defence system. SOD, which has a crucial defensive role against

oxidative stress in the body, transforms the superoxide anion free radical (O₂⁻) into its less reactive H₂O₂ form. H₂O₂, which is a significant sensor in the redox metabolism, is transformed by GSH-Px into H₂O, and thus, H₂O₂ accumulation is prevented [59–60]. In our study, we determined that exposure to arsenic decreased SOD and GSH-Px enzyme activities in BALB/c 3T3 fibroblasts. In *in vivo* and *in vitro* studies, arsenic exposure caused a decrease in SOD and GSH-Px activities, whereas antioxidant supplementation increased these activities [30, 54, 56, 57, 61, 62]. Decreased SOD and GSH-Px activity may also be associated with arsenic toxicity due to increased production of superoxide radical ions and H₂O₂. Quercetin administration may upregulate SOD and GSH-Px enzyme activity by neutralising or reducing arsenic toxicity. Our findings support the view that arsenic significantly affects the enzymes that metabolise ROS and antioxidant enzymes such as SOD and GSH-Px [28]. In addition to triggering lipid peroxidation in membranes, arsenic triggers protein synthesis by binding to carbonyl groups [50, 63–64]. The most commonly used marker to assess protein oxidation is protein carbonylation, and the most commonly used marker to assess lipid peroxidation is MDA. MDA is considered the most mutagenic product because DNA can react with nitrogen bases [65, 66]. In our study, similar to its determination in embryonic lung fibroblast and adrenal gland cells, it was found to have significantly increased lipid peroxidation. High lipid peroxidation levels are suggested to be due to increased levels of free radicals that directly attack polyunsaturated fatty acids in the cell membrane [28, 59, 67]. PC increase that accompanies an increase in MDA and a decrease in SOD and GSH-Px activities are suggestive of accumulating superoxides and peroxides [68]. These findings show that arsenic can significantly reduce the activity of antioxidant enzymes such as SOD, GSH-Px, but increase the level of oxidative agents such as MDA and PC, leading to oxidative damage. In addition to being an effective ROS scavenger and reducing agent, quercetin displays antioxidant effects by accelerating the activation of antioxidant enzymes and inhibiting lipid peroxidation [69].

Quercetin's antioxidant effect and its strong ability to clean free radicals and bind to the transition metal ions in terms of its scavenging free radicals are due to the existence of two antioxidant pharmacophores in its structure [70–71]. In our study, quercetin support decreased MDA and protein carbonyl contents in the cell line, and the increase in SOD and GSH-Px activities decreased arsenic load significantly. Quercetin appears to have a beneficial effect on reducing arsenic-induced oxidative stress, as supported by observed changes in antioxidant enzyme activity and cell damage indicators.

In vivo and in vitro studies have shown that exposure to specific arsenic types can increase the expression of TNF- α and IL-1 β proinflammatory cytokines [72–73]. Proinflammatory cytokines participate in the upregulation of inflammatory reactions. Although arsenic increased TNF- α and IL-1 β levels in our study, quercetin reduced the inflammation. These results are consistent with those of previous studies. Increasing ROS in our data suggests its relationship with the inflammatory process [74–75]. This result shows that arsenic exposure has negative effects on inflammation and that quercetin may have potential protective effects against these inflammatory processes. These results highlight quercetin's potential to protect against inflammation and highlight the need for further studies on such effects.

Arsenic-induced apoptosis is also free radical-mediated. In this context, arsenic is considered a well-established apoptosis inducer [76]. Under oxidative damage, some proteins act as redox switches, stabilising other protein ranges to maintain band signaling. Excessive oxidation leads to the destruction of protein thiols, leading to structural instability and ultimately cell death [77]. For instance, arsenic has been demonstrated to induce apoptosis in peripheral blood mononuclear cells and Chinese hamster ovarian cells [78]. Consistent with studies reporting that arsenic exposure induces apoptotic cell death in various cellular systems, we demonstrated that arsenic exposure induces cell death [79]. In contrast, quercetin provides a protective role against arsenic-induced toxicity by regulating apoptosis-related changes (Bax, Bcl-2 and Caspase-3). In the study, regarding cell apoptosis determined through the TUNEL method, while the apoptotic cell count peaked in different doses of arsenic, almost no apoptotic cells were determined in the control group and quercetin group. Nevertheless, the apoptotic cell count that increased with arsenic significantly decreased with quercetin. Furthermore, our RT-PCR results showed that arsenic increased Caspase-3 and Bax mRNA expression and decreased Bcl-2 mRNA expression. In contrast, quercetin Caspase-3 and Bax decreased mRNA expression, whereas Bcl-2 expression increased. (Fig. 6A and B). In a study conducted, it was shown that 2 μ M arsenic could induce apoptosis

dose-dependently in U87MG, U251, SHG44, and C6 glioma cells [80]. A previous study showed that 2 μ M arsenic can induce apoptosis dose-dependently in U87MG, U251, SHG44, and C6 glioma cells [80]. These data suggest that exposure to arsenic can accelerate apoptotic processes at the cellular level, whereas quercetin can inhibit such processes. In another study conducted in which rat C6 and 9 L cell sequences were used, it was demonstrated that 5 μ M arsenic trioxide strongly prevented cell viability and induced apoptosis by downregulating Bcl-2 expression and upregulating Bax expression [81]. Based on evidence of the protective effects of both curcumin and D-pinitol against arsenic toxicity, Rahman et al. observed upregulated expression of proapoptotic Bax and Caspase-3 and downregulated expression of anti-apoptotic Bcl-2 after arsenite (As³⁺) exposure in PC12 cells [55]. They reported that curcumin alone or in combination with D-pinitol effectively suppressed apoptotic cell death induced by As³⁺.

In this molecular docking study, which we know was evaluated for the first time by us, the relationship between arsenic and quercetin in fibroblast cells was molecularly revealed. While quercetin bound to the fibroblast cell structure with a good binding structure with a docking score of -6.6 kcal/mol, the binding score of arsenic to the fibroblast cell structure was bound to a low score of -2.4 kcal/mol. The reason why arsenic binds with a low score is due to the hydrophobic interactions of the amino acid bonds (VAL106, TYR107, LEU116, ALA134, PHE136) in its structure. Additionally, quercetin and arsenic were similarly bound to the amino acid ALA134. Quercetin contributes to the high docking score by forming hydrogen bonds with GLY43 and ARG131. Molecular docking results showed that quercetin bound very well to GSH-Px and SOD enzyme structures, which are important in the oxidative damage process. Quercetin bound to the GSH-Px structure with molecular binding scores of -6.8 kcal/mol and to the SOD structure with molecular binding scores of -6.6 kcal/mol. On the other hand, it was determined that quercetin showed a good binding affinity to Bax, Bcl2 and Caspase-3 structures, which are important in the apoptosis process. quercetin was bound to the Bax structure with molecular docking scores of -7.5 kcal/mol, to the Bcl-2 structure -7.7 kcal/mol and to the caspase-3 structure of -6.2 kcal/mol. Quercetin showed good binding affinity to the target region in TNF- α and IL-1 β protein structures, which are important in the inflammatory process.

DMSA or succimer, an analog of BAL (dimercaptopropanol), contains two carboxylic groups and two thiol groups, along with thiol groups that participate in the metal-ligand reaction. Compounds such as dihydroliipoic acid, BAL, DMPS, and succimer are used to treat lead, mercury, and arsenic toxicity, and these compounds

Table 5 H-bond and hydrophobic interaction between high binding score Quercetin

Target Protein	Quercetin H-bond	Quercetin Hydrophobic
4S00-Bax	GLU41, GLU42, ARG134	ALA46, ILE133
2AZ5-TNF- α	-	PRO139, ASP140, PHE144
1CBJ-SOD	THR86, ILE94, VAL98	VAL85, ILE97
2XYG-Caspase-3	LYS105, LYS138, PHE142, ARG147	ASN141
1GP1- Glutathione Peroxidase	PRO103	ALA21, LEU89, GLU102
1ITB-IL-1 β	SER5, ASN7, LYS63, PRO87, TYR90	GLU64, PRO91
1G5M-Bcl-2	TRP195	ASN182, HIS186, ILE189

Table 6 Comparison of predictive models parameters properties of Quercetin and succimer

		Quercetin	Succimer
Physicochemical Properties	MW	302.24 g/mol	182.22 g/mol
	Formula	C15H12O	C4H6O4S2
	Num. rotatable bonds	1	3
	Num. H-bond acceptors	7	4
	Num. H-bond donors	5	2
Lipophilicity	Molar Refractivity	78.03	40.74
	Topological polar surface area (TPSA)	131.36 Å ²	152.20 Å ²
	Log Po/w (XLOGP3)	1.54	0.06
Solubility	Log $P_{o/w}$ (WLOGP)	1.99	-0.25
	Log $P_{o/w}$ (MLOGP)	-0.56	-0.54
	Log S (ESOL)	-3.16	-0.81
	Solubility	2.11e-01 mg/ml; 6.98e-04 mol/l	2.83e+01 mg/ml; 1.55e-01 mol/l
Druglikeness	Class	Soluble	Very soluble
	Lipinski (RO5)	Yes; 0 violation	Yes; 0 violation
	Ghose	Yes	No; 1 violation: #atoms<20
	Veber	Yes	No; 1 violation: TPSA>140
	Egan	Yes	No; 1 violation: TPSA>131.6
Leadlikeness	Bioavailability Score	0.55	0.11
	Synthetic accessibility	3.23	2.66

are the most effective chelating antidotes. The FDA has approved DMSA for treating lead poisoning in paediatric patients [82–85]. To the best of our knowledge, we are the first study to compare the drug properties of quercetin and succimer using computer-based calculations (Tables 5 and 6). Quercetin is a good drug candidate.

Table 7 Comparison of Pharmacokinetic properties of Quercetin and succimer

		Quercetin	Succimer
Pharmacokinetics	GI absorption	High	Low
	BBB permeant	No	No
	P-gp substrate	No	No
	CYP1A2 inhibitor	Yes	No
	CYP2C19 inhibitor	No	No
	CYP2C9 inhibitor	No	No
	CYP2D6 inhibitor	Yes	No
	CYP3A4 inhibitor	Yes	No
	Log Kp (skin permeation)	-7.05 cm/s	-7.37 cm/s
	Allergenicity (CHAI Pred)	Score 0.21 Non-allergen	0.3 Non-allergen

GI (HIA) = Human gastrointestinal absorption, BBB = Blood-brain barrier permeation P-gp = Permeability glycoprotein, Log Kp = Theskin permeability coefficient

Considering its higher synthetic accessibility score, better pharmacokinetic properties, and good biological transition and interaction capacities, quercetin can be considered a more beneficial and effective compound. On the other hand, succimer shows limited efficacy with a lower biomolecular interaction potential and higher TPSA; This suggests that it may have limited efficacy in biological systems. The inhibition and induction of CYPs are the main mechanisms causing pharmacokinetic drug-drug interactions. The important CYPs CYP1A2, CYP2C19, CYP3A4, CYP2C9, and CYP2D6 are particularly analysed in in silico analyses [86–87]. By CYP interaction, succimer was not inhibitory for CYP1A2, CYP2C19, CYP2C9, CYP2D6, and CYP3A4, whereas quercetin was inhibitory for CYP1A2, CYP2D6, and CYP3A4. When succimer is used, it is unlikely to produce any adverse or unexpected effects on the effects of drugs metabolised through these enzymes, whereas when quercetin is used, it is likely to affect the metabolism of existing drugs and increase the effects or side effects of drugs metabolised through these enzymes. In particular, because CYP3A4 is the major metabolic pathway for many drugs, it is important to consider potential interactions with quercetin on this enzyme (Table 7).

Conclusion

Arsenic increases MDA and PC levels by increasing oxidative stress and reduces the activity of antioxidant enzymes such as SOD and GSH-px. Therefore, arsenic damages cell membranes and proteins. Arsenic also increases proinflammatory cytokines and apoptotic proteins. Quercetin increases antioxidant capacity by reducing ROS production in cells, and it has the potential to reduce arsenic toxicity by maintaining a balance between inflammation and apoptosis. These findings

suggest quercetin is an effective and safe therapeutic agent against arsenic toxicity in biological systems. Furthermore, further *in vivo* and *in vitro* studies may provide useful information on the effects of quercetin on other environmental toxicants. In molecular docking analyses, we observed that the hydrogen bonds formed by quercetin with amino acid structures in fibroblast cells helped to achieve a strong binding score and could suppress the negative effects caused by arsenic. *In vitro* results revealed the benefits of quercetin in reducing arsenic-induced oxidative stress, which was supported by changes in antioxidant enzyme activity and cell damage indicators.

Abbreviations

ANOVA	One-way analysis of variance
Bax	Bcl-2-associated X protein
Bcl-2	B-cell lymphoma 2
CYPs	Cytochromes P450
DAPI	4',6-diamidino-2-phenylindole
DMSA	2,3-Dimethylmercaptosuccinic Acid
ELISA	Enzyme-Linked ImmunoSorbent Assay
GSH-Px	Glutathione peroxidase
IL-1 β	Interleukin 1 beta
LGA	Lamarckian Genetic Algorithm
LDH	Lactate dehydrogenase
MDA	Malondialdehyde
PC	Protein carbonyl
ROS	Reactive Oxygen Species
SMILES	Simplified Molecular Line Entry System
SOD	Superoxide dismutase
TPSA	Topological Polar Surface Area
TNF- α	Tumor necrosis factor- α

Acknowledgements

The English language check was carried out by Dr. Ahmet Butun, we thank him.

Author contributions

Velid Unsal: Project administration, Formal analysis, Conceptualization, Investigation, Methodology, Supervision, Visualization, Writing – original draft, Writing – review & editing. Cumali Keskin: Investigation, Methodology, Writing – original draft, Erkan Oner: Methodology, Investigation, Formal analysis, Conceptualization, Writing – original draft.

Funding information

No.

Data availability

The data that support the findings of this study are available from the corresponding author upon reasonable request.

Declarations

Ethical approval

This research does not require ethical approval. The study did not include any human or animal participants that required consent to participate and/or publish findings.

Publication approval

All authors have approved the article and declared that it is an original contribution and that no material in this article has been considered for publication elsewhere.

Competing interests

The authors declare no competing interests.

Author details

¹Department of Nutrition and Dietetics, Faculty of Health Sciences, Mardin Artuklu University, Mardin, Türkiye

²Department of Medical Services and Techniques, Vocational School of Health Services, Mardin Artuklu University, Mardin, Türkiye

³Department of Biochemistry, Faculty of Pharmacy, Adiyaman University, Adiyaman, Türkiye

Received: 19 April 2024 / Accepted: 17 March 2025

Published online: 25 March 2025

References

- Mannerström M, Toimela T, Sarkanen JR, Heinonen T. Human BJ fibroblasts is an alternative to mouse BALB/c 3T3 cells in *in vitro* neutral red uptake assay. Volume 121. *Basic & Clinical Pharmacology & Toxicology*; 2017. pp. 109–15.
- Rahimi AM et al. 2022. Heterogeneity of the NIH3T3 Fibroblast Cell Line. *Cells*. 28;11(17):2677. <https://doi.org/10.3390/cells11172677>
- Boncler M, et al. Differentiated mitochondrial function in mouse 3T3 fibroblasts and human epithelial or endothelial cells in response to chemical exposure. *Basic Clin Pharmacol Toxicol*. 2019;124(2):199–210.
- Mandal BK, Suzuki KT. Arsenic round the world: a review. *Talanta*. 2002;58(1):201–35.
- Wang S, Mulligan CN. Occurrence of arsenic contamination in Canada: sources, behavior and distribution. *Sci Total Environ*. 2006;366(2–3):701–21.
- Hu Y, Li J, Lou B, Wu R, Wang G, Lu C, Xu Y. The role of reactive oxygen species in arsenic toxicity. *Biomolecules*. 2020;10(2):240.
- Carlin DJ, Naujokas MF, Bradham KD, Cowden J, Heacock M, Henry HF, Suk WA. Arsenic and environmental health: state of the science and future research opportunities. *Environ Health Perspect*. 2016;124(7):890–899.
- Shi H, Shi X, Liu KJ. Oxidative mechanism of arsenic toxicity and carcinogenesis. *Mol Cell Biochem*. 2004;255:67–78.
- Flora SJS, Dube SN, Arora U, Kannan GM, Shukla MK, Malhotra PR. Therapeutic potential of meso 2, 3-dimercaptosuccinic acid or 2, 3-dimercaptopropane 1-sulfonate in chronic arsenic intoxication in rats. *Biometals*. 1995;8:111–6.
- Garkal A, Sarode L, Bangar P, Mehta T, Singh DP, Rawal R. Understanding arsenic toxicity: implications for environmental exposure and human health. *J Hazard Mater Lett*. 2024;5:100090.
- Khan SS, Sharma A, Flora SJ. Phytochemicals in the management of arsenic toxicity. *Chem Res Toxicol*. 2022;35(6):916–34.
- Nath P, Priyadarshni N, Chanda N. Europium-coordinated gold nanoparticles on paper for the colorimetric detection of arsenic (III, V) in aqueous solution. *ACS Appl Nano Mater*. 2017;1(1):73–81.
- Hrycak EG, Bandiera SM. Involvement of cytochrome P450 in reactive oxygen species formation and cancer. *Adv Pharmacol*. 2015;74:35–84.
- Martinez VD, Vucic EA, Adonis M, Gil L, Lam WL. (2011). Arsenic biotransformation as a cancer promoting factor by inducing DNA damage and disruption of repair mechanisms. *Mol Biol Int*. 2011(1):718974.
- Martinez VD, Becker-Santos DD, Vucic EA, Lam S, Lam WL. Induction of human squamous cell-type carcinomas by arsenic. *J Skin Cancer*. 2011(1):454157.
- Susan A, Rajendran K, Sathyasivam K, Krishnan UM. An overview of plant-based interventions to ameliorate arsenic toxicity. *Biomed Pharmacother*. 2019;109:838–52.
- Balakumar P, Kaur J. Arsenic exposure and cardiovascular disorders: an overview. *Cardiovasc Toxicol*. 2009;9:169–76.
- Abraham MJ, Murtola T, Schulz R, Páll S, Smith JC, Hess B, Lindahl E. GRO-MACS: high performance molecular simulations through multi-level parallelism from laptops to supercomputers. *SoftwareX*. 2015;1:19–25.
- Shaker B, Ahmad S, Lee J, Jung C, Na D. Silico methods and tools for drug discovery. *Comput Biol Med*. 2021;137:104851.
- Acharyya N, Chattopadhyay S, Maiti S. Chemoprevention against arsenic-induced mutagenic DNA breakage and apoptotic liver damage in rat via antioxidant and SOD1 upregulation by green tea (*Camellia sinensis*) which recovers broken DNA resulted from arsenic-H2O2 related *in vitro* oxidant stress. *J Environ Sci Health Part C*. 2014;32(4):338–61.
- Singh PK, Chakrabarty D, Dwivedi S, Kumar A, Singh SP, Sinam G, Tripathi RD. Nitric oxide-mediated alleviation of arsenic stress involving metalloid detoxification and physiological responses in rice (*Oryza sativa* L.). *Environ Pollut* 2022;297:118694.

22. Zubair M, Ahmad M, Qureshi ZI. Review on arsenic-induced toxicity in male reproductive system and its amelioration. *Andrologia*. 2017;49(9):e12791.
23. Koyama H, Kamogashira T, Yamasoba T. Heavy metal exposure: molecular pathways, clinical implications, and protective strategies. *Antioxidants*. 2024;13(1):76.
24. Kannan GM, Flora SJ. Chronic arsenic poisoning in the rat: treatment with combined administration of succimers and an antioxidant. *Ecotoxicol Environ Saf*. 2004;58(1):37–43.
25. Miller AL. Dimercaptosuccinic acid (DMSA), a non-toxic, water-soluble treatment for heavy metal toxicity. *Altern Med Review: J Clin Therapeutic*. 1998;3(3):199–207.
26. Priyadarshni N, Nath P, Nagahnumaiah, Chanda N. DMSA-functionalized gold Nanorod on paper for colorimetric detection and Estimation of arsenic (III and V) contamination in groundwater. *ACS Sustain Chem Eng*. 2018;6(5):6264–72.
27. Bhattacharya S, Haldar PK. *Trichosanthes dioica* fruit ameliorates experimentally induced arsenic toxicity in male albino rats through the alleviation of oxidative stress. *Biol Trace Elem Res*. 2012;148:232–41.
28. Singh G, Thaker R, Sharma A, Parmar D. Therapeutic effects of Biochanin A, Phloretin, and epigallocatechin-3-gallate in reducing oxidative stress in arsenic-intoxicated mice. *Environ Sci Pollut Res*. 2021;28:20517–36.
29. Cicek M, Unsal V, Doganer A, Demir M. Investigation of oxidant/antioxidant and anti-inflammatory effects of apigenin on apoptosis in sepsis-induced rat lung. *J Biochem Mol Toxicol*. 2021;35(5):e22743.
30. Slika, Hasan, et al. Therapeutic potential of flavonoids in cancer: ROS-mediated mechanisms. *Biomed Pharmacother*. 2022;146:112442.
31. Andres S, Pevny S, Ziegenhagen R, Bakhiya N, Schäfer B, Hirsch-Ernst KI, Lampen A. Safety aspects of the use of Quercetin as a dietary supplement. *Mol Nutr Food Res*. 2018;62(1):1700447.
32. Xu D, et al. Antioxidant activities of quercetin and its complexes for medicinal application. *Molecules*. 2019;21;24(6):1123.
33. Serban MC, et al. Lipid and blood pressure Meta-analysis collaboration (LBPMC) group. Effects of Quercetin on blood pressure: a systematic review and meta-analysis of randomized controlled trials. *J Am Heart Association*. 2016;5(7):e002713.
34. D'Andrea G. Quercetin: A flavonol with multifaceted therapeutic applications? *Fitoterapia*. 2015;106:256–71.
35. Liu Y, Tang ZG, Lin Y, Qu XG, Lv W, Wang GB, Li CL. Effects of Quercetin on proliferation and migration of human glioblastoma U251 cells. *Biomed Pharmacother*. 2017;92:33–8.
36. Batiha GES, Beshbishy AM, Ikram M, Mulla ZS, El-Hack MEA, Taha AE, Elewa YHA. The pharmacological activity, biochemical properties, and pharmacokinetics of the major natural polyphenolic flavonoid: quercetin. *Foods*. 2020;9(3):374.
37. Bule M, et al. Antidiabetic effect of Quercetin: A systematic review and meta-analysis of animal studies. *Food Chem Toxicol*. 2019;125:494–502.
38. Sun Y. A simple method for clinical assay of superoxide dismutase. *Clin Chem*. 1988;34(3):497–500.
39. Paglia DE, Valentine WN. Studies on the quantitative and qualitative characterization of erythrocyte glutathione peroxidase. *J Lab Clin Med*. 1967;70(1):158–69.
40. Esterbauer H, Cheeseman KH. Determination of aldehydic lipid peroxidation products: malonaldehyde and 4-hydroxynonenal. *Methods in enzymology*. Academic. 1990:186;407–21.
41. Levine RL. Determination of carbonyl content in oxidatively modified proteins. *Methods Enzymol*. *Methods in Enzymology* Edited by Packer L, Glazer AN. Orlando, Fla, Academic Press. 1990:464–478.
42. Lowry O, et al. Rosebrough Nj, Farr al, Randall Rj. Protein measurement with the Folin phenol reagent. *J Biol Chem*. 1951;193(1):265–75.
43. Oner E, et al. Investigation of Berberine and its derivatives in Sars Cov-2 main protease structure by molecular docking, PROTOX-II and ADMET methods: in machine learning and in Silico study. *J Biomol Struct Dynamics*. 2023;41(19):9366–81.
44. Pandey RK, et al. Structure-based virtual screening, molecular docking, ADMET and molecular simulations to develop Benzoxaborole analogs as potential inhibitor against leishmania donovani trypanothione reductase. *J Recept Signal Transduction*. 2017;37(1):60–70.
45. Sathishkumar N. Molecular Docking studies of anti-apoptotic BCL-2, BCL-XL, and MCL-1 proteins with ginsenosides from *Panax ginseng*. *J Enzyme Inhib Med Chem*. 2012;27(5):685–92.
46. BIOVIA DS. Dassault Systèmes BIOVIA, Discovery Studio, 2019, San Diego: Dassault Systèmes. San Diego. 2016. Retrieved from <https://www.3dsbiovia.com/about/citations-references/>
47. Daina A. SwissADME: a free web tool to evaluate pharmacokinetics, drug-likeness and medicinal chemistry friendliness of small molecules. *Sci Rep*. 2017;7:42717.
48. Erkes DA, Selvan SR. Hapten-induced contact hypersensitivity, autoimmune reactions, and tumor regression: plausibility of mediating antitumor immunity. *J Immunol Res*. 2014;2014(1):175265.
49. Sharma N, Patiyal S, Dhall A, Devi NL, Raghava GP. ChAIPred: a web server for prediction of allergenicity of chemical compounds. *Comput Biol Med*. 2021;136:104746.
50. Liao WT, Chang KL, Yu CL, Chen GS, Chang LW, Yu HS. Arsenic induces human keratinocyte apoptosis by the FAS/FAS ligand pathway, which correlates with alterations in nuclear factor- κ B and activator protein-1 activity. *J Invest Dermatol*. 2004;122(1):125–9.
51. Chen CJ. Health hazards and mitigation of chronic poisoning from arsenic in drinking water: Taiwan experience. *Rev Environ Health*. 2014;29(1–2):13–9.
52. Taheri M, et al. High soil and groundwater arsenic levels induce high body arsenic loads, health risk and potential anemia for inhabitants of Northeastern Iran. *Environ Geochem Health*. 2016;8(2):469–82.
53. Kumar P, et al. Analysis of cell viability by the lactate dehydrogenase assay. *Cold Spring Harb Protoc*. 2018;20186:465–8.
54. Perker MC, et al. Protective effects of Curcumin on biochemical and molecular changes in sodium arsenite-induced oxidative damage in embryonic fibroblast cells. *J Biochem Mol Toxicol*. 2019;33(7):e22320.
55. Rahman MM, et al. Ameliorative effects of selenium on arsenic-induced cytotoxicity in PC12 cells via modulating autophagy/apoptosis. *Chemosphere*. 2018;196:453–466. <https://doi.org/10.1016/j.chemosphere.2017.12.149>
56. Rahaman MS. Effects of Curcumin, D-pinitol alone or in combination in cytotoxicity induced by arsenic in PC12 cells. *Food Chem Toxicol*. 2020;144:111577.
57. Orta YB, et al. Sodium arsenite-induced detriment of cell function in Leydig and Sertoli cells: the potential relation of oxidative damage and antioxidant defense system. *Drug Chem Toxicol*. 2020;43(5):479–87.
58. Chen L, et al. Protection afforded by Quercetin against H₂O₂-induced apoptosis on PC12 cells via activating PI3K/Akt signal pathway. *J Recept Signal Transduction*. 2016;36(1):98–102.
59. Unsal V, et al. Toxicity of carbon tetrachloride, free radicals and role of antioxidants. *Rev Environ Health*. 2021;36(2):279–95.
60. Rosa AC, et al. Superoxide dismutase administration: A review of proposed human uses. *Molecules*. 2021;25(7):1844.
61. Zhao Z, Li J, Zheng B, Liang Y, Shi J, Zhang J, Gao Y. Ameliorative effects and mechanism of crocetin in arsenic trioxide-induced cardiotoxicity in rats. *Mol Med Reports*. 2020;22(6):5271–5281.
62. Xu M, Rui D, Yan Y, Xu S, Niu Q, Feng G, Jing M. Oxidative damage induced by arsenic in mice or rats: a systematic review and meta-analysis. *Biol Trace Elem Res*. 2017;176:154–175.
63. Manna P, et al. Protection of arsenic-induced testicular oxidative stress by Arjunolic acid. *Redox Rep*. 2008;13(2):67–77.
64. Momeni HR, Eskandari N. Effect of Curcumin on kidney histopathological changes, lipid peroxidation and total antioxidant capacity of serum in sodium arsenite-treated mice. *Exp Toxicol Pathol*. 2017;69(2):93–7.
65. Unsal V. Natural phytotherapeutic antioxidants in the treatment of mercury intoxication—a review. *Adv Pharm Bull*. 2018;8(3):365. <https://doi.org/10.15171/apb.2018.043>
66. Weber D, et al. Determination of protein carbonyls in plasma, cell extracts, tissue homogenates, isolated proteins: focus on sample Preparation and derivatization conditions. *Redox Biol*. 2015;5:367–80.
67. Flora SJ. Arsenic-induced oxidative stress and its reversibility. *Free Radic Biol Med*. 2011;51(2):257–81.
68. Unsal V, Kolkucu E, Gevrek F, Firat F. Sinapic acid reduces ischemia/reperfusion injury due to testicular torsion/detorsion in rats. *Andrologia*. 2021;53(8):e14117.
69. Tang SM, Deng XT, Zhou J, Li QP, Ge XX, Miao L. Pharmacological basis and new insights of Quercetin action in respect to its anti-cancer effects. *Biomed Pharmacother*. 2020;121:109604.
70. Islam MR, et al. In silico QSAR analysis of quercetin reveals its potential as therapeutic drug for Alzheimer's disease. *J Young Pharmacists*. 2013;5(4):173–9.
71. Boots AW, et al. Health effects of quercetin: from antioxidant to nutraceutical. *Eur J Pharmacol*. 2008;585(2–3):325–37.

72. Das S, et al. Implications of oxidative stress and hepatic cytokine (TNF- and IL-6) response in the pathogenesis of hepatic collagenesis in chronic arsenic toxicity. *Toxicol Appl Pharmacol*. 2005;204(1):18–26.
73. Zhang M, et al. AIM2 inflammasome mediates Arsenic-induced secretion of IL-1 B and IL-18. *Oncoimmunology*. 2016;5(6):e1160182.
74. Ahmed S, et al. Arsenic-Associated oxidative stress, inflammation, and immune disruption in human placenta and cord blood. *Environ Health Perspect*. 2011;119(2):258–64.
75. Unsal V, Koluoku E, Firat F, Gevrek F. The protective effects of sinapic acid on acute renal ischemia/reperfusion injury. *Turkish J Biochem*. 2021;46(5):563–71. <https://doi.org/10.1515/tjb-2021-0115>
76. Roy S, et al. Arsenic-induced instrumental genes of apoptotic signal amplification in death-survival interplay. *Cell Death Discovery*. 2016;2(1):1–6.
77. Tripathi S. Therapeutic effects of CoenzymeQ10, Biochanin A and Phloretin against arsenic and chromium induced oxidative stress in mouse (*Mus musculus*) brain. *3 Biotech*. 2022;12(5):116.
78. de la Fuente H, et al. Effect of arsenic, cadmium and lead on the induction of apoptosis of normal human mononuclear cells. *Clin Experimental Immunol*. 2002;129(1):69–77.
79. Mu YF, et al. Arsenic compounds induce apoptosis through caspase pathway activation in MA–10 Leydig tumor cells. *Oncol Lett*. 2019;18(1):944–54.
80. Cheng Y, Li Y, Ma C, Song Y, Xu H, Yu H, Zhao G. Arsenic trioxide inhibits glioma cell growth through induction of telomerase displacement and telomere dysfunction. *Oncotarget*. 2016;7(11):12682.
81. Sun Y, Wang C, Wang L, Dai Z, Yang K. Arsenic trioxide induces apoptosis and the formation of reactive oxygen species in rat glioma cells. *Cell Mol Biol Lett*. 2018;23:1–10.
82. Aaseth J, et al. Chelation therapy in the treatment of metal intoxication. Academic 2016. ISBN: 978-0-12-803072-1. <https://doi.org/10.1016/C2014-0-01302-0>
83. Flora S. Chelation in metal intoxication. *Int J Environ Res Public Health*. 2010;7:2745–88.
84. Kim JJ, Kim YS, Kumar V. Heavy metal toxicity: an update of chelating therapeutic strategies. *J Trace Elem Med Biol*. 2019;54:226–31.
85. Nurchi VM, et al. Arsenic toxicity: molecular targets and therapeutic agents. *Biomolecules*. 2020;10(2):235.
86. Lynch T, Price A. The effect of cytochrome P450 metabolism on drug response, interactions, and adverse effects. *Am Fam Physician*. 2007;76:391–6.
87. Hakkola J. Inhibition and induction of CYP enzymes in humans: an update. *Arch Toxicol*. 2020;94:3671–722.

Publisher's note

Springer Nature remains neutral with regard to jurisdictional claims in published maps and institutional affiliations.